SMAR 2017 – Fourth Conference on Smart Monitoring,
Assessment and Rehabilitation of Civil Structures

SMAR 2017

New anchorage mechanism for smooth Fe-SMA bar used for flexural strengthening of RC beams using NSM technique

Hothifa Rojob[1] and Raafat El-Hacha[1]

[1] University of Calgary, Department of Civil Engineering, Calgary, Alberta, Canada

ABSTRACT: Self-prestressing using Iron-based Shape Memory Alloy (Fe-SMA) bars/strips is emerging as a potential practical system for strengthening of reinforced concrete (RC) beams. For flexural strengthening of RC beams using the Near-Surface Mounted (NSM) technique, the Fe-SMA bars/strips are inserted in a groove on the tension side of the RC beam and then activated through heating. The heating triggers the Fe-SMA to apply prestressing force to the beam, hence reduces deflection and cracking. In this paper, a new way of anchoring the NSM Fe-SMA bar to the RC beam is discussed and compared to anchorage systems used elsewhere in the literature.

1 INTRODUCTION

The Iron-based Shape Memory Alloys (Fe-SMA) have been used recently by several researches for strengthening of RC beams. Soroushian et al. (2001) was the first to use Fe-SMA bars for external prestressing for shear strengthening of bridge girders. Cladera et al. (2014) in their literature review paper, highlighted the potential capabilities of the Fe-SMA materials in the field of prestressing applications. Rojob and El-Hacha (2017a) used 14.3 mm diameter smooth NSM Fe-SMA bars for flexural strengthening of 2.0 m long RC beams. They reported a significant improvement in the flexural capacity at service and ultimate limit states of the beams strengthened with Fe-SMA bars over the control unstrengthened beam. More importantly, the strengthened beams failed in a ductile failure mode by crushing of concrete after the yielding of the steel and Fe-SMA materials. Similar observations were reported by Shahverdi et al. (2016a, 2016b) In their research work, deformed NSM Fe-SMA bars and strip were used to strengthen 2.5 m RC beams. Rojob and El-Hacha (2016) and El-Hacha and Rojob (2017) used NSM Fe-SMA strips to strengthen large-scale RC beam. The tested beams were 5.0 m long and were strengthened with different number of self-prestressed NSM Fe-SMA strips. The results of beams strengthened with NSM Fe-SMA strips were compared to similar beams strengthened with prestressed NSM Carbon FRP (CFRP) strips with comparable prestressing forces. While the beams strengthened with NSM Fe-SMA strips attained comparable ultimate and service loads as the prestressed NSM CFRP-strengthened beams, the beams strengthened with Fe-SMA strips maintained a ductile behavior similar to the control unstrengthened beam. On the other hand, the CFRP-strengthened beams failed in brittle failure mode by rupture of the FRP strips prior to the crushing of concrete. Rojob and El-Hacha (2015a, 2016) presented a numerical comparison between small scale (2.0 m long) and large-scale (5.0 m long) RC beams strengthened with prestressed NSM CFRP rods and similar beams strengthened using self-prestressing NSM Fe-SMA strips. Both techniques show a similar performance at the service load conditions. While the beams strengthened with prestressed NSM

CFRP rods show strength-ductility trade-off, the beams strengthened with NSM Fe-SMA strips exhibited more ductile behaviour, this is attributed to the pseudo-yielding nature of the Fe-SMA.

In order to induce the prestressing force in the Fe-SMA bars, the bars need to be restrained during the activation process, i.e. heating. Two different restraining mechanisms were used by researchers. Rojob and El-Hacha (2017a) and El-Hacha and Rojob (2017) used end anchors to transfer the prestressing force to the RC beams as illustrated in Figure 1. After the Fe-SMA bars were anchored to the beams, the bars were then heated directly as presented in Figure 2, and the grout was filled in the groove after the bars cooled down. On the other hand, Shahverdi et al. (2016a, 2016b) didn't use end anchors, rather, they relied completely on the bond between the NSM Fe-SMA bar/strip and the surrounding grout to transfer the prestressing force to the concrete beam. Therefore, they first inserted the Fe-SMA material inside the grooves, then the grooves were filled with grout and finally the Fe-SMA bars/strips were heated using resistive heating (through electric current). An illustration of the heating process conducted by Shahverdi et al. (2016a, 2016b) is shown in Figure 3. In the former case, the Fe-SMA bars/strips were smooth (with no surface finishing), therefore, the bond between the grout and the Fe-SMA material wouldn't be strong enough to transfer the prestressing force. While in the latter case, the Fe-SMA strips/bars were ribbed.

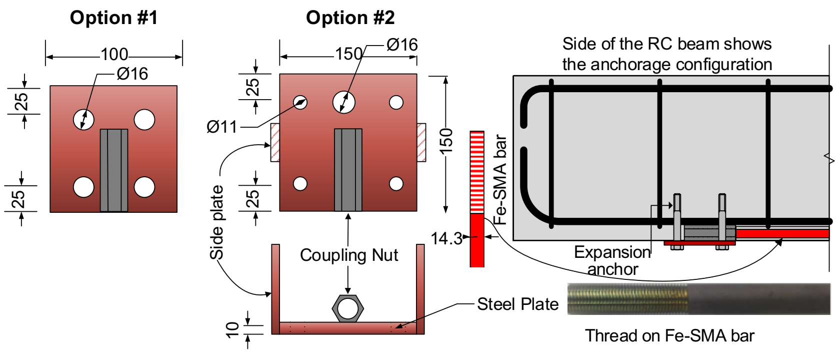

Figure 1. Anchors used by Rojob and El-Hacha (2015c, 2015b, 2015d, 2017a, 2017c) and El-Hacha and Rojob (2015)

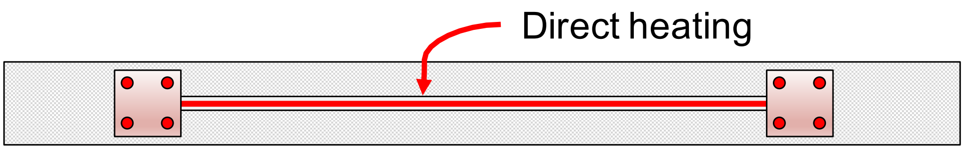

Figure 2. Heating process used by Rojob and El-Hacha (2015b, 2016, 2017a, 2017c) and El-Hacha and Rojob (2015).

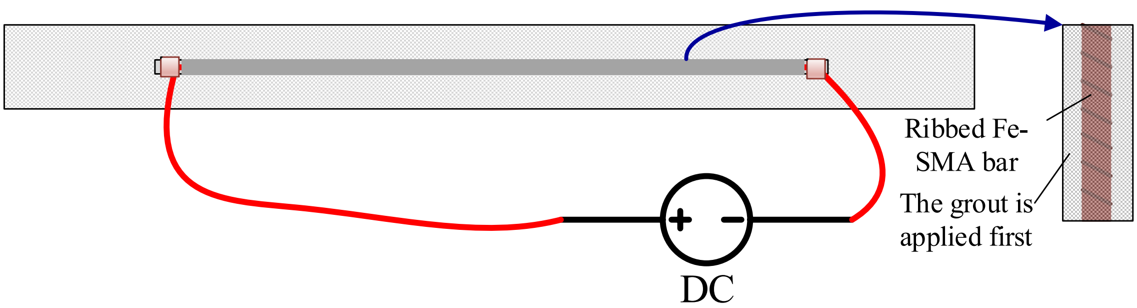

Figure 3. Heating process used by Shahverdi et al. (2016a, 2016b).

The surface of the Fe-SMA bar used in the current project is smooth, similar to those used by Rojob and El-Hacha (2017a), therefore, it is crucial to provide end anchors. A different type of end anchors is proposed herein.

2 EXPERIMENTAL PROGRAM

The experimental program included testing two 2.0 m long RC beams with cross sectional dimensions of 305×150 mm. One beam was strengthened with 1.3 m long NSM Fe-SMA bar (Beam SMA-1), while the other beam was used as a control unstrengthened beam. Both beams were tested monotonically under four-point bending setup until failure.

2.1 Specimens' details

The two beams were designed according to CSA A23.3-14 (2014) as under-reinforced beams. The concrete compressive strength of a cylinder at 28 days was 39.1 MPa tested according to ASTM C39 (2017). The beams were reinforced with two 15M bars in tension and two 10M bars in compression with a total steel cross-sectional area of 400 mm^2 and 200 mm^2, respectively. The specified yield strength of the steel reinforcements was 400 MPa. Two-legged 10M closed steel stirrups were placed at a spacing of 150 mm to prevent shear failure. Figure 4 shows the geometric details of the strengthened beam (Beam SMA-1), and the loading setup. The beam was instrumented with 7 Strain Gauges (SG); two of them were mounted on the tension steel reinforcements at the mid-span and 5 were mounted along the Fe-SMA bar. Three Linear Strain Conversion transducers (LSC) were mounted on the side of the beam at the mid-span to measure strains: one at the level of the tension, one at the level of compression steel, and one at the mid height of the beam. Two laser transducers were used to monitor the deflection at the mid-span.

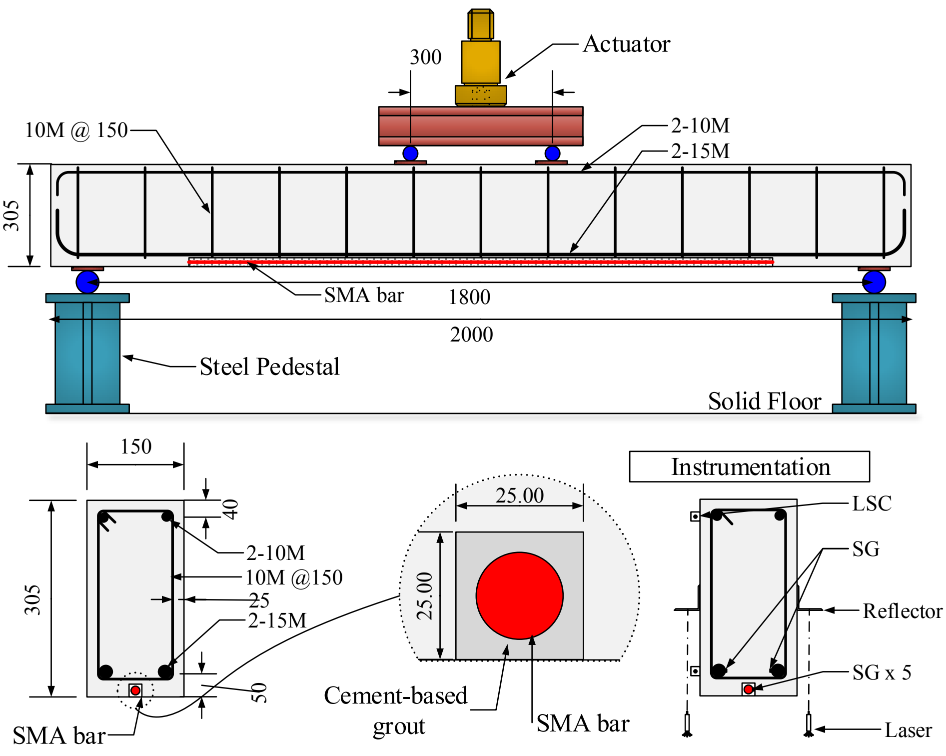

Figure 4. Details of the strengthened beam (Beam SMA-1).

2.2 Fe-SMA material characteristics

The Fe-SMA bar used herein was produced by Awaji (2014). The bar was 14.3 mm in diameter with a smooth surface. The tensile behavior of the Fe-SMA bar was tested and the stress-strain curve is shown in Figure 5.

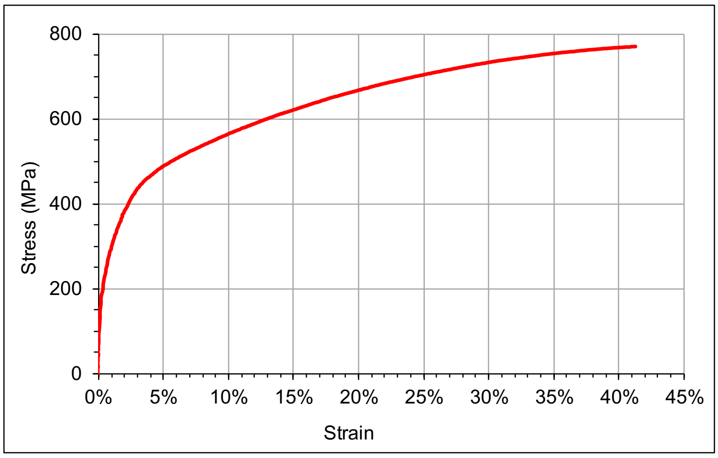

Figure 5. Stress-strain behavior of the Fe-SMA bar Rojob and El-Hacha (2015b, 2016, 2017a, 2017b) and El-Hacha and Rojob (2017).

The Shape Memory Effect (SME) properties of the Fe-SMA bar was reported by Rojob and El-Hacha (2015b, 2017b). The recovery stress (the stress developed in the pre-strained Fe-SMA bar when heated while restrained at both ends) is plotted against temperature as shown in Figure 6.

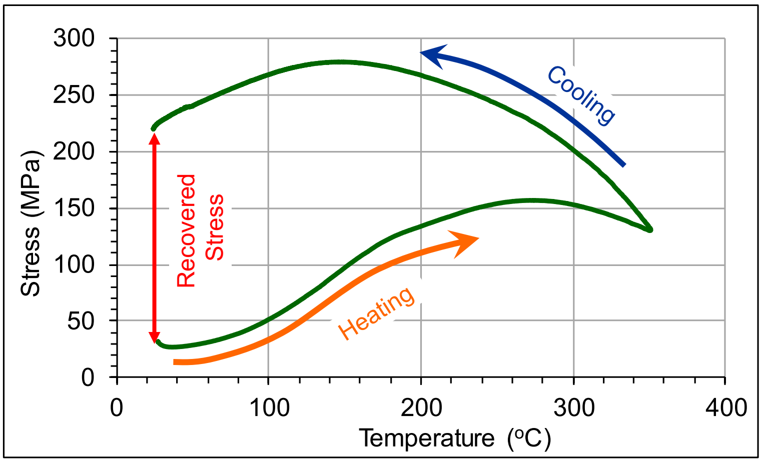

Figure 6. The Shape Memory Effect (SME) of the Fe-SMA bar (Rojob and El-Hacha 2015b, 2017b).

2.3 Strengthening procedure:

2.3.1 Anchorage system

A schematic drawing of the anchorage mechanism is shown in Figure 7. The 1.3m long bar was bent 90° angle at both ends, the ends were then inserted into 18 mm diameter and 170 mm deep pre-drilled holes in the bottom side of the RC beam, leaving a 960mm straight bar. The holes were then filled with Sikadur 330 epoxy adhesive (Sika, 2012a). In such a way, the bracket-type anchorage system shown in Figure 1 was eliminated. Further, after filling the groove, no exposed parts of the system can be seen.

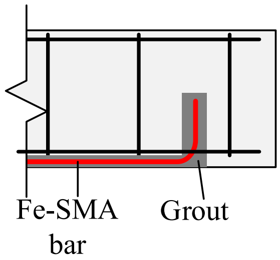

Figure 7. schematic drawing of the end anchor.

2.3.2 Heating

After the Fe-SMA bar was anchored to the beams using the proposed anchorage mechanism explained above, the bar was then directly heated using an oxy-acetylene rosebud torch. The change of strain in the tension steel was measured during the heating process as an indirect way to monitor the effect of the prestressing force that developed in the Fe-SMA bar. After the bar cooled to room temperature, 5 strain gauges were mounted along the bar to measure strain in the bar during the loading stage. The groove was then filled with SikaGrout 428 (Sika, 2012b).

3 RESULTS

3.1 Prestressing stage

During the heating process, the strain in the 15M tension steel reabars was reported. Figure 8 shows the change in the tension steel strain at the mid-span of the strengthened beam (SMA-1) and another beam (SMA-2) tested by Rojob and El-Hacha (2015b, 2017b). Both beams had the same configuration, except the end anchors. In beam SMA-1, the proposed end anchor described in Figure 7 was used, while in beam SMA-2, the anchor in Figure 1 (option #1) was used. It can be noticed that there was a drop in the strain at the beginning of the heating process which was more evident in beam SMA-1. Any drop in the strain implies an imperfection of the end anchors, which eventually leads to a reduction of the amount of prestressing force transferred to the beam.

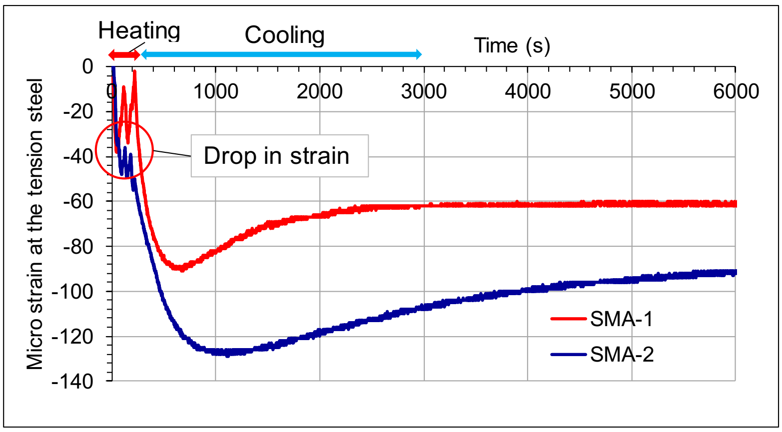

Figure 8. Change of strain in tension steel during the heating process (results of beam SMA-2 from Rojob and El-Hacha (2015b, 2017b)).

3.2 Flexural test

The RC beams were tested on a four-point bending setup to failure as presented earlier in Figure 4. The load versus mid-span deflection curves of the control beam and the strengthened beam is shown in Figure 9. The strengthened beam experienced better performance at service and ultimate load conditions. The cracking and ultimate loads of the strengthened beam was 20% and 18% higher than the control beam, respectively. Both beams failed by crushing of concrete after the yielding of the steel reinforcements. No failure or cracks were noticed at the end anchor's location.

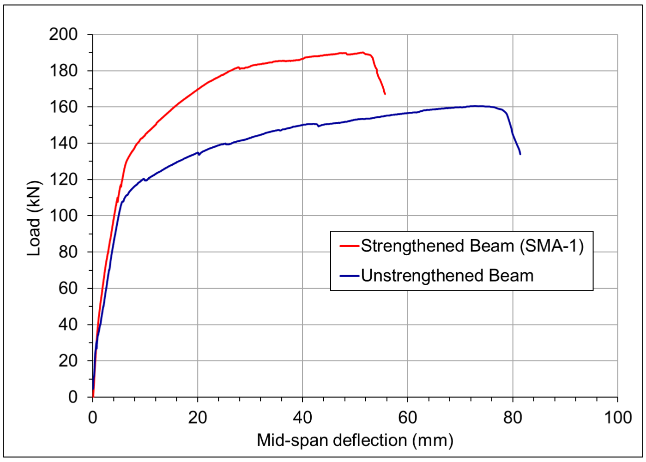

Figure 9. Load deflection curves of the strengthened and the control beams.

Table 1. Summary of the testing results

Beam	Unstrengthened Beam	Strengthened Beam	%Δ
Cracking load: P_{cr}, kN	30.5	36.7	20.3
Yielding load: $P_{y,}$ kN	103	128	24.3
Ultimate load: P_u, kN	160.5	190	18.3
Deflection at yielding: Δ_y, mm	5.2	6.2	19.2
Deflection at ultimate: Δ_u, mm	72.8	51.3	-29.5

The NSM Fe-SMA bar maintained good contact with the grout until debonding occurred at about the yielding load as presented in Figure 10. This reflects the adequacy of SikaGrout 428 in maintaining good bond with the Fe-SMA bar under service loads. Figure 11 shows the strain distribution along the Fe-SMA bar at diffident loading stages. At the load 150 kN, it can be noticed that the strain at the mid-span is equal to the strain at the strain gauge 250 mm to the left of it. This also implies that a debonding occurred in that region.

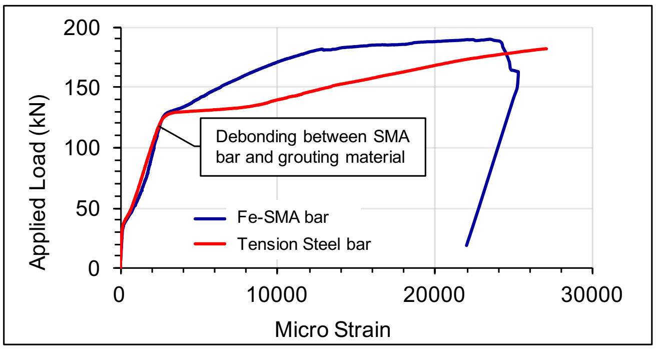

Figure 10. Strain versus load in Fe-SMA bar and steel bar at the mid-span of the beam.

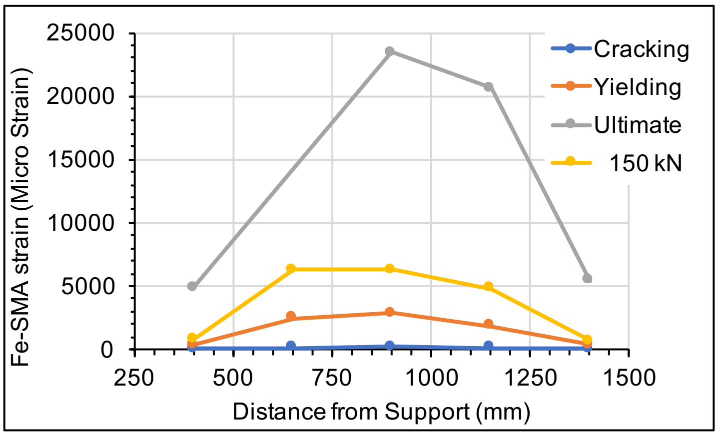

Figure 11. Strain along the Fe-SMA bar at different loading stages. Note: the strain gauge number 2 from left failed prior to the ultimate load.

4 CONCLUSIONS

A new anchorage mechanism was proposed and used to anchor NSM Fe-SMA bar to the tension face of the RC beam without the need to use steel brackets and bolts. The ends of the Fe-SMA bar were bent 90^{o} and inserted into a pre-drilled 170 mm holes. The holes were then filled with epoxy adhesive. During the activation process, it was noticed that there has been some sort of anchorage setting which resulted in a reduction in the prestressing force. The anchorage mechanism maintained good contact at the anchor locations through the flexural test, where no failure or cracks were noticed at these anchorage locations. The strengthened beam attained higher service and ultimate load carrying capacities compared to the control unstrengthened beam. More research is needed to investigate the adequacy of this system under fatigue loading.

5 ACKNOWLEDGMENTS

The authors would like to acknowledge the University of Calgary and NSER for the financial support toward this research project. In addition, the authors acknowledge the laboratory technicians at the structural engineering lab at the University of Calgary as well Mr. Mouhammad Amiri (MSc student at the University of Calgary) and Mr. Xiuyin Deng (an exchange student at the University of Calgary form Harbin Institute of Technology in China) for their help in conducting the experiments.

6 REFERENCES

ASTM International, (2017), "Standard test method of compressive strength of cylindrical concrete specimens", *ASTM C39/C39M-17*, Vol. 4.02, American Society for Testing Material, West Conshohocken, PA, USA

Awaji. (2014). "Shape Memory Alloys". [cited 2014 1 January]; Available from: http://www.awaji-m.jp/english/r_and_d/about.html.

Cladera, A., Weber, B., Leinenbach, C., Czaderski, C., Shahverdi, M., Motavalli, M. (2014). "Iron-based shape memory alloys for civil engineering structures: An overview". *Construction and Building Materials*, 63, 281-293.

CSA-A23.3-14, (2014), "Design of concrete structures", Canadian Standard Associations, Ontario, Canada, 2014.

El-Hacha, R., Rojob, H. (2015). "Fatigue Performance of RC Beams Strengthened in Flexure Using NSM Iron-Based Shape Memory Alloy Bars". *Proceedings of the 3rd International Conference on Smart Monitoring, Assessment and Rehabilitation of Civil Structures* (SMAR 2015), Antalya, Turkey, 7-9 September 2015. 8p.

El-Hacha, R., Rojob, H. (2017). "Flexural Strengthening of Large-Scale RC Beams Using Near-Surface Mounted Self-Prestressed Iron-Based Shape Memory Alloy Strips". *PCI journal*, "Submitted".

Rojob, H., El-Hacha, R. (2015a). "Numerical Investigation of the Flexural Performance of RC Beam Strengthened With Iron-Based Shape Memory Alloy Bar". *Proceedings of the Concrete Innovations: Research Into Practice* (Concrete 2015), Melbourne, Australia, August 30–September 2, 2015. 7p.

Rojob, H., El-Hacha, R. (2015b). "Ductility behavior of RC beams strengthened in flexure with NSM Iron-based Shape Memory Alloy bars". *Proceeding of the 3rd Conference on Smart Monitoring, Assessment and Rehabilitation of Civil Structures* (SMAR 2015), Antalya, Turkey, September 7-9, 2015. 8p.

Rojob, H., El-Hacha, R. (2015c). "Flexural Strengthening of RC Beam Using NSM Iron-Based Shape Memory Alloys". *Proceedings of the 4th International Conference on Concrete Repair, Rehabilitation and Retrofitting* (ICCRRR 2015), Leipzig, Germany, October 05-07, 2015. 8p.

Rojob, H., El-Hacha, R. (2015d). "Thermo-Mechanical Training of Iron-Based Shape Memory Alloys Used to Strengthen RC Beams". *Proceedings of the 5th International Workshop on Performance, Protection & Strengthening of Structures under Extreme Loading* (PROTECT 2015), East Lansing, Michigan, USA, June 29-30, 2015, pp. 382-389.

Rojob, H., El-Hacha, R. (2016). "Prestressed CFRP for Flexural Strengthening of RC Beams versus Self-Prestressing SMA – A Comparison". *Proceedings of the 8th International Conference on FRP Composites in Civil Engineering* (CICE 2016), Hong Kong, China, December 14-16, 2016. USP-6p.

Rojob, H., El-Hacha, R. (2017a). "Self-Prestressing Using Iron-Based Shape Memory Alloy for Flexural Strengthening of Reinforced Concrete Beams". *ACI Structural J.*, 114 (2), 523-532.

Rojob, H., El-Hacha, R. (2017b). "Performance of RC beams strengthened with self-prestressed Fe-SMA bars exposed to freeze-thaw cycles and sustained load". *Journal of Engineering Structures*, "Submitted".

Rojob, H., El-Hacha, R. (2017c). "Fatigue performance of RC beams strengthened with self-prestressed iron-based shape memory alloys". *Journal of Engineering Structures*, "Submitted"

Shahverdi, M., Czaderski, C., Annen, P., Motavalli, M. (2016a). "Strengthening of RC beams by iron-based shape memory alloy bars embedded in a shotcrete layer". *Engineering Structures*, 117, 263-273.

Shahverdi, M., Czaderski, C., Motavalli, M. (2016b). "Iron-based shape memory alloys for prestressed near-surface mounted strengthening of reinforced concrete beams". *Construction and Building Materials*, 112, 28-38.

SIKA. (2012a). "Product Data Sheet: Sikadur 330 (Sika Inc.)". [cited 2016 October 9]; Available from: https://can.sika.com/.

SIKA. (2012b). "Product Data Sheet: SikaGrout 428 (Sika Inc.)". [cited 2016 October 9]; Available from: https://can.sika.com/.

Soroushian, P., Ostowari, K., Nossoni, A., Chowdhury, H. (2001). "Repair and strengthening of concrete structures through application of corrective posttensioning forces with shape memory alloys". *Transport Res Rec*, 1770, 20-26.